



Usage of Yb(OH)CO₃ Nanoparticles-based Computed Tomography Image in the Prediction Model of Lung Biopsy Pneumothorax

Wei Hu^{1#}, Jing Hu^{2#}, Wei Guo¹, Jun Chen¹, Shuang Liang¹, Wei Qian¹, Xi Yuan^{1*}

¹Department of Radiology, The Fifth Hospital of Wuhan, Wuhan, 430050, China

²Department of Aspiration Medicine, Wuhan University Hospital, Wuhan, 430071, China

#These authors contributed equally to this work as co-first author

ARTICLE INFO

ABSTRACT

Original paper

Article history:

Received: November 02, 2021

Accepted: March 06, 2022

Published: March 31, 2022

Keywords:

computed tomography (CT)
contrast, lung biopsy
pneumothorax, nanoparticles,
prediction model, Yb(OH)CO₃

This study aimed to explore the application of Yb(OH)CO₃ nanoparticles in the prediction model of computed tomography (CT) contrast lung biopsy pneumothorax (LBP) by synthesizing a new type of Yb(OH)CO₃ nanoparticles, which provides a basis for clinical application. Yb(OH)CO₃ nanoparticles were prepared by a homogeneous precipitation process based on urea, and the samples were characterized by scanning electron microscopy (SEM) and transmission electron microscopy (TEM). Methyl thiazolyl tetrazolium (MTT) assay was adopted in vitro cytotoxicity test, optical density (OD) value was measured with a microplate reader at a wavelength of 570 nm, the cell viability was analyzed, and the cytomorphological changes were observed with an optical microscope. Besides, 40 selected patients with CT-guided percutaneous needling biopsy (PTNB) were rolled into a control group and an observation group. A pneumothorax prediction model was constructed under the support vector machine (SVM) model. The accuracy, sensitivity, and specificity of SVM for pneumothorax prediction were 88.7%, 71.3%, and 100%, respectively; while those of CT imaging with Yb(OH)CO₃ nanoparticles were 96.7%, 84.3%, and 100%, respectively. Mean squared errors (MESs) of Yb(OH)CO₃ nanoparticles-based CT contrast agent and conventional contrast agent were 14,532 and 7,021, respectively, and mutual information (MI) was 0.1232 and 0.2354, respectively, so the difference between the two groups was significant ($P < 0.05$). In summary, Yb(OH)CO₃ nanoparticles-based CT contrast agents showed good histocompatibility and low toxicity, and the Yb(OH)CO₃ nanoparticles-based CT images showed high accuracy in the prediction of LBP.

DOI: <http://dx.doi.org/10.14715/cmb/2022.68.3.29>

Copyright: © 2022 by the C.M.B. Association. All rights reserved.



Introduction

The incidence of lung cancer is remarkably increasing, especially in some industrialized countries (1-3). According to the latest statistical analysis data of lancet, the survival rate of patients with lung cancer for 5 years is very low. From 2005 to 2009, the 5-year survival rate for lung cancer in Europe and American countries were both lower than 20%. In contrast, that in Asian countries was much lower, and it was even as low as 7%-9% in Mongolia and Thailand. In China, the 5-year survival rate for lung cancer reached 7.5% between 1995 and 1999, while that between 2000 and 2004 amounted to 18.1%. From 2005 to 2009, the 5-year survival rate for lung cancer was 17.5% (4,5). According to the global statistical data released in 2018, lung cancer is one of the commonest tumors worldwide. The number of new cases with lung cancer was about 2.09 million, and the number of

death cases reached about 1.76 million, accounting for 11.6% of the total number of new cases with malignant tumors and 18.4% of that of death cases with malignant tumors, respectively. Two values were ranked in the first place among the number of new patients with different types of malignant tumors and that of dead patients with different types of malignant tumors, respectively (6). According to domestic data statistics, lung cancer is not only the commonest malignant tumor in China, but it is also the primary cause of the death of domestic patients with malignant tumors. Patients who died from malignant tumors accounted for 23.91% of all domestic residents who died from different diseases National cancer statistical data released domestically in January 2019 showed that the number of new cases of lung cancer in China in 2015 reached about 0.787 million with the incidence being 57.26/0.1 million. In addition, the

*Corresponding author. E-mail: cheguainao265@163.com
Cellular and Molecular Biology, 2022, 68(3): 258-269

number of patients dying from lung cancer was about 0.631 million with the mortality reaching 45.87/0.1 million (7). The high mortality and low 5-year survival rate were caused mainly by the failure in early detection and diagnosis, the heterogeneity of tissue typing, and the lack of a profound and thorough understanding of the molecular mechanism in the tumorigenic progression. To reduce the high mortality caused by lung cancer, enhance the 5-year survival rate of patients, and improve the living quality during patient prognosis, the early detection and diagnosis of lung cancer were of great significance (8). Because of the lack of the clinical manifestations of specificity of lung cancer, most patients suffered from metastatic diseases with poor diseases when diagnosed with lung cancer clinically. Hence, the increase in the diagnosis rate of lung cancer could diagnose patients with lung cancer as early as possible, prolong patients' survival time, improve the survival quality of patients, and benefit patients. Therefore, it is vital to enhance the diagnosis rate of lung cancer.

Computerized tomography (CT) is an effective method of lung cancer screening. The greatest research achievement so far was published in 2011. In this experiment, the mortality of patients during the screening of patients with lung cancer in the chest X-ray examination group and lung low-dose CT group was compared. The results of the study showed that the mortality of patients in the lung low-dose CT group was reduced by 20.0% compared with that in the chest X-ray examination group among the high-risk population (9). CT-guided lung biopsy pneumothorax (LBP) was an effective method of the diagnosis of pathological diagnosis of lung lesions. It was reported that the accuracy of CT-guided percutaneous lung biopsy could reach 64%-97% (10). Besides, the incidence of its complications was very high at the initial stage of the adoption of the technical method, amounting to 61%. The commonest complication of LBP is pneumothorax. Because lung tumor tissue is very close to normal tissue density, the utilization of a CT contrast agent is necessary to realize better CT imaging effects. However, most CT contrast agents for clinical use are iodine compounds with high X-ray absorption coefficients. Freely moving iodized small-molecule compounds contact frequently vascular walls. When the vascular walls in the human body or cells in other tissues are allergic to

iodine, allergic reactions occur among patients injected with contrast agents. Besides, drugs flow through the body via blood after small-molecule drugs enter the human body. Because the radius of small-molecule particles in drugs is too small, most of the particles leak from vascular sides into the gaps in extra-vascular tissues or are removed by the kidney quickly. The leakage and the removal of small-molecule drugs exert toxic and side effects on normal tissues and organs. What's more, the drug concentration in target tissues can't reach imaging concentration. Therefore, the amount of drugs injected into the human body usually needs to be increased to obtain ideal imaging effects. In this case, the human body is negatively harmed more seriously. New imaging contrast agents with longer imaging time, better imaging effects, and few side effects and new tumor treatment methods are the hot topics in present research, development, and exploration.

With the development of bionanotechnology, nanoprobe-based CT contrast agents are expected to overcome the above shortcomings (11-13). Because the small-sized nanoparticle matches the size of biomolecules, it can be adopted as a contrast agent to detect the pathology in the body. Besides, it also can be utilized to design nanoprobe that can manipulate biological functions (14). Compared with traditional small-molecule contrast agents, nanoparticles can load a large number of imaging elements. Nanoparticles result in long blood circulation, and low renal clearance as well as capillary leakage rate. Furthermore, they can passively accumulate at tumor positions by the high permeability and retention of solid tumors (15). By different surface modifications, nanoparticles can also acquire the function of active targeting, or treatment and multi-modal imaging. Iodine is adopted as the imaging element in the nano-CT contrast agents firstly prepared. Iodide was made into nano-emulsion or embedded into carriers to enhance blood circulation time and biocompatibility. At present, the metal-based nanomaterial is widely applied in the studies on CT contrast agents, which are based on its unique physical, chemical, and biological features. Rabin et al. (2006) (16) adopted Bi₂S₃ nanocrystals modified by polyvinylpyrrolidone in CT imaging of living blood vessels, livers, and lymph nodes. The results of the study demonstrated that Bi₂S₃ nanomaterial enhanced the detection sensitivity

and accuracy. Meanwhile, it reduced the dosage of contrast agents and improved toxic and side effects. The metal ytterbium (Yb) is a rare earth element with a rich electronic structure, and it shows many optical, electrical, and magnetic properties. With a high operating voltage (120KVp), Yb can offer a high degree of X-ray attenuation. The voltage CT machines adopt is usually 120KVp. After the nanocrystallization of Yb, it demonstrates many properties, such as small size effect, high specific effect, quantum effect, extremely strong optical, electrical, and magnetic properties, and chemical activity whose superconductivity is much higher than that of conventional substances. Nano-Yb can enhance the performance and function of materials greatly and can be utilized to produce multiple-function materials. It is a new research direction in current CT contrast agents. However, there are little research data on nano-Yb at present. Based on this, Yb(OH)CO₃ nanoparticles were prepared by a homogeneous precipitation process and their representation was analyzed in the research. After that, the cytotoxicity of Yb(OH)CO₃ nanoparticles was studied by in vitro experiment. Besides, the pneumothorax prediction model was constructed by a support vector machine (SVM), and the effects and puncture accuracy of CT imaging adopting Yb(OH)CO₃ nanoparticles were discussed to offer references to the optimization of puncture path to reduce the incidence of pneumothorax by clinicians in the research.

Materials and methods

Preparation methods of Yb(OH)CO₃ nanoparticles

Yb(OH)CO₃ nanoparticles were prepared by homogeneous precipitation method, which was based on urea in the research. In the experimental process, the utilized reagents, including urea (CH₄N₂O) and ethyl alcohol (C₂H₆O), were both analytically pure. The main methods of preparing Yb(OH)CO₃ nanoparticles were explained as follows. With the growth of temperature, urea could be decomposed as OH⁻ and CO₃²⁻. As a result, it could be used as a metal ion precipitator. Yb(NO₃)₃·5H₂O (7.5mmol) and urea (15g) were dissolved into deionized water, and the total volume of the solution reached 500mL. Then, the solution was stirred until it became uniform. At room temperature, the above solution was stirred by

magnetic stirring apparatus for 2 hours to make it become uniform. After that, the acquired uniform solution was bathed in oil at 90°C for 3 hours. Then, the obtained suspension liquid was separated by centrifugation. Next, the obtained product, which was a white powder, was wrapped by gauze and placed into a Soxhlet extractor. After being washed with deionized water three times, it was washed with ethyl alcohol three times. Finally, it was stored in a vacuum at thermostatic 60°C for 24 hours for subsequent experimental study. Figure 1 showed the preparation technical process below.

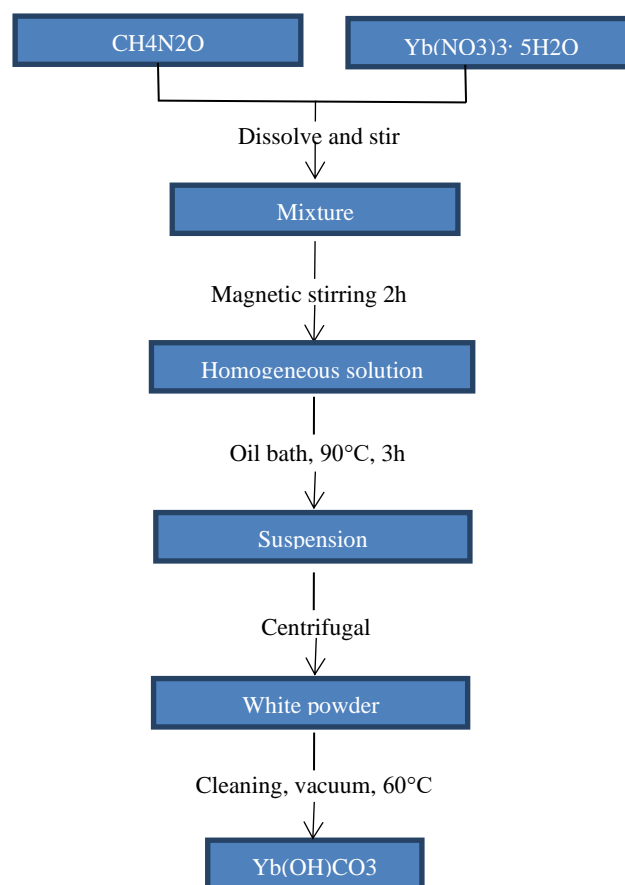


Figure 1. The preparation process of Yb(OH)CO₃ nanoparticles.

Morphology representation of prepared Yb(OH)CO₃ nanoparticles

Scanning electron microscopy (SEM) was usually utilized to observe the morphology, structure, and components of nanomaterials. Its operating principle was the selection of very narrow electron beams to scan specimens. Trigger actions occurred between electron beams and substances, which generated scattered electrons, secondary electrons, and

transmission electrons. The physical information of the samples could be obtained by generated electronic signals. Next, the information was converted into images by systems to present relevant information, including the composition and morphology of samples. Consequently, the adoption of SEM could not only observe the surface features of different nanomaterials but also could help obtain more three-dimensional and morphological features with a wider range of observation. In the research, S-3700N SEM was utilized to observe the micro-morphology of Yb(OH)CO₃ nanoparticles, and the operation voltage was set to 25KV.

The operation principle of transmission electron microscopy (TEM) was very similar to that of general microscopes in many aspects. In general, the light source of optical microscopes was natural light, and the lens was made of transparent glass. In contrast, TEM adopted the electron beams with short wavelengths as the light source. Because a shorter wavelength meant stronger penetrability, the scattering of substances was more significant. The electromagnetic field is the lens of TEM. Electron beams were transmitted to the tested samples, and then atoms collided and interacted with others to generate different solid angle scattering. After that, different specimens produced various images due to their different density and crystal structure. Hence, TEM could be adopted to obtain the crystal orientation and structure of the selected areas. What's more, selected area electron diffraction was also utilized. In the research, HI-TACHIH-800 TEM was utilized to observe the structure of Yb(OH)CO₃ nanoparticles.

Cytotoxicity of Yb(OH)CO₃ nanoparticles

Hepatoma carcinoma cells (HePG2) were selected and utilized in the research, and cell lines were provided by The Fifth Hospital of Wuhan. Before the cell experiment, the prepared Dulbecco's modified eagle medium (DMEM) cell culture medium (10% fetal calf serum+1% anti-body), phosphate buffer solution (PBS), 0.25% of trypsin, and Yb(OH)CO₃ cell suspension were placed into a super clean bench for ultraviolet ray sterilization for 1 hour. Meanwhile, culture flasks and centrifugal tubes adopted in the experiment were sterilized at high temperatures in advance. After that, HePG2 cells were extracted from

liquid nitrogen tanks at -80°C and then shaken constantly in a water bath cauldron at 37°C to dissolve them completely within 1 minute. After that, they were centrifuged at 1,000rpm for 5 minutes and then added with the proper amount of complete culture medium. After that, they were percussed evenly and the cell suspension was transferred into culture flasks. Then, they were cultured at 37°C in cell thermostatic incubators containing 5% CO₂. The routine culture was performed after the fluid was changed every other day. Cells growing into the log phase were taken and inoculated into 96-well cell culture plates at the density of 5×10³cells/wells. Next, they were placed at 37°C in thermostatic incubators containing 5% CO₂ overnight. When the cell density reached 80%, Yb(OH)CO₃ nanoparticle suspension with the final concentration of 0 μg/mL, 20 μg/mL, 50 μg/mL, 75 μg/mL, and 100 μg/mL were added into the 96-well plates. In each group, there were 3 compound wells, and Yb(OH)CO₃ nanoparticle suspension was cultured for 48 hours. After the culture, each well was added with a 10μL methyl thiazolyl tetrazolium (MTT) solution. Next, they were incubated in cell culture incubators for 4 hours. After 4 hours, each well was added with 100μL Formazan solving liquid and mixed properly. After that, they were continued to be incubated in cell incubators until formazan was completely dissolved by the observation under a general optical microscope. Then, an enzyme-labeled instrument was adopted to measure the absorbance (optical density) at the wavelength of 570nm. Equation (1) was utilized to calculate the cell survival rate below. Besides, the changes in cell morphology were observed by an optical microscope.

$$\text{cell survival rate} = \frac{\text{OD}_{\text{experiment}}}{\text{OD}_{\text{control}}} \times 100\% \quad [1]$$

Toxicity of Yb(OH)CO₃ nano contrast agents in mice body

In the research, 20 mice were selected randomly and divided into 2 groups. Appropriate humidity as well as temperature, and single cage feeding were offered to mice 1 week before the experiment. The feeding and management of mice conformed to the standards of the Animal Ethics Committee. 10 of the selected mice were injected with normal saline and included in the control group, and the rest of the 10 mice were injected with the prepared Yb(OH)CO₃

nanoparticle suspension and included in the experimental group. The dosage of the injected the above liquid was 20mg NPs/kg. The dissected mice were sacrificed 30 days after the experiment, and then the toxicity of Yb(OH)CO₃ was analyzed by hematoxylin (HE) staining analysis.

Construction of pneumothorax prediction models

The construction methods of pneumothorax prediction models in the research were based on the published articles with slight modifications. Figure 2 demonstrated the specific process of constructing the model. The process was divided into three steps. In the preprocessing step, data sets were normalized. In the feature extraction step, the features most related to the incidence of pneumothorax were detected. The most effective feature was found from the original features to optimize the prediction precision and reduce feature dimensions. The prediction step was based on SVM and other machine learning models to train the sample data and construct pneumothorax prediction models. In addition, whether patients would suffer from pneumothorax was predicted. Meanwhile, the reinforcement learning (RF) model was compared with the SVM model. The quantitative evaluation of the constructed models was implemented with the sensitivity, specificity, and accuracy being adopted as the indexes.

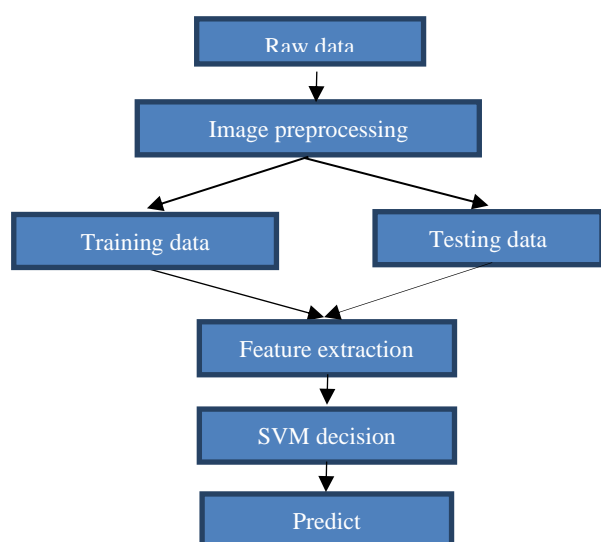


Figure 2. SVM prediction model process.

Research objects of LBP

A total of 40 patients receiving CT-guided percutaneous needling biopsy (PTNB) at The Fifth

Hospital of Wuhan were selected for the research. Among all the selected patients, there were 26 males and 14 females aged between 35 and 79. All the patients were divided into 20 observation groups (CT imaging adopting Yb(OH)CO₃ nanoparticles) and control groups (conventional CT imaging) according to random numbers. The implementation of the research had been approved by The Fifth Hospital of Wuhan Ethics Society. Besides, all patients and their family members had been informed of the research and signed the informed consent forms. The cases were included in the research based on the following standard. The clinical data and imaging data of patients were both complete. The cases were excluded from the research based on the following standard. The maximum diameter of patients' lesions was less than 5mm, and patients suffered from a mental disorder or conscious disturbance.

Lung puncture biopsy

In the research, the 16-slice spiral CT scanner of American General Electric Company was adopted. The scanning parameters were set as follows. Tube voltage was 120kV, tube current was 120mAs, scanning layer thickness, and spacing was both 2mm. Patients were placed in the supine or prone position. Besides, the body surface puncture point, angle, and depth were determined at the workstation, and then they were marked on the body surface. Next, the body surface puncture point was sterilized, covered with towels, infiltrated, and anesthetized locally with 1% lidocaine. After that, 18G coaxial biopsy needles were pierced into lesions along the predetermined puncture route, and then samples were extracted twice in different positions of lesions combined with cutting needles and automatic biopsy guns. After the surgery, needles were withdrawn, and chest CT scanning was performed to observe if pneumothorax and hemorrhage occurred after the puncture point was compressed and bound up. Finally, the imaging effects of CT imaging and puncture accuracy in the observation group and control group were compared.

Results and discussion

Morphological features of Yb(OH)CO₃

Yb(OH)CO₃ nanoparticles were prepared by the homogeneous precipitation method. Figure 3 showed the results of SEM and TEM of Yb(OH)CO₃

nanoparticles below. Figure 3I and Figure 3II demonstrated that the obtained Yb(OH)CO₃ nanoparticles after preparation were spherical with the average diameter reaching about 170nm. Each Yb(OH)CO₃ nanoparticle had a clear boundary, and its surfaces were smooth with excellent dispersibility.

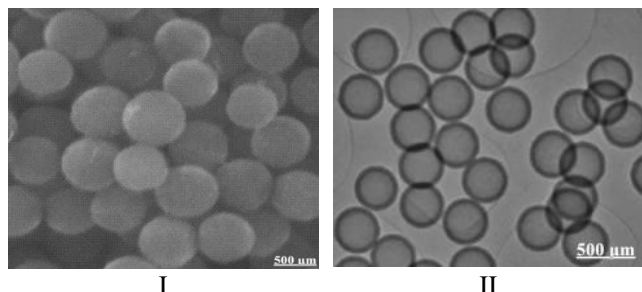


Figure 3. SEM and TEM diagrams of prepared Yb(OH)CO₃ nanoparticles. (Figure I represented the SEM diagram of Yb(OH)CO₃ nanoparticles, and Figure II displayed the TEM diagram of Yb(OH)CO₃ nanoparticles)

Influences of Yb(OH)CO₃ nanoparticles on HePG2 cell morphology

Figure 4 presented the morphology of HePG2 cells processed by 100 µg/mL Yb(OH)CO₃ nanoparticles. According to Figure 4, the proliferation of cells in Figure 4I and Figure 4II was significant, and they were diffused outward. Besides, the morphology of cells added with 100 µg/mL Yb(OH)CO₃ nanoparticles was not inhibited compared with that in the blank control group (without being added with Yb(OH)CO₃ nanoparticles), while the diffusion of cells added with 100 µg/mL Yb(OH)CO₃ nanoparticles was close to that in the control group. The results of the above comparisons demonstrated that Yb(OH)CO₃ nanoparticles with the highest concentration in the research had little influence on the morphology of HePG2 cells.

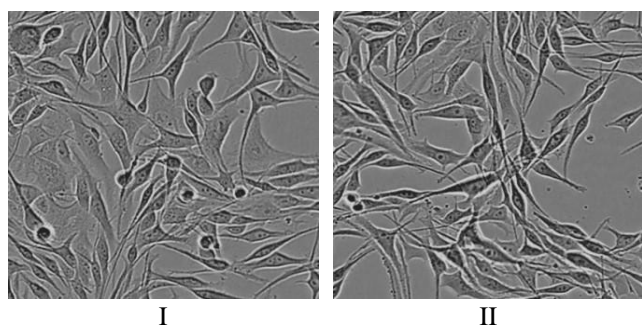


Figure 4. HePG2 cell morphology. (Figure I represented the blank control group, and Figure II presented the status of cells added with 100µg/mL Yb(OH)CO₃ nanoparticles)

Influences of Yb(OH)CO₃ nanoparticles on HePG2 cell viability

The role of Yb(OH)CO₃ nanoparticles in HePG2 cell viability was studied by the MTT experiment, and Figure 5 demonstrated the results of the experiment. According to Figure 5, the growth of cells was not inhibited after the culture of HePG2 cells with Yb(OH)CO₃ nanoparticles being added. The cell morphology was still long spindle. Besides, the cell viability level was above 92% when the concentration of Yb(OH)CO₃ nanoparticles amounted to 200 µg/mL. The results revealed that the toxicity of the prepared Yb(OH)CO₃ nanoparticles in the research for HePG2 cells was very low.

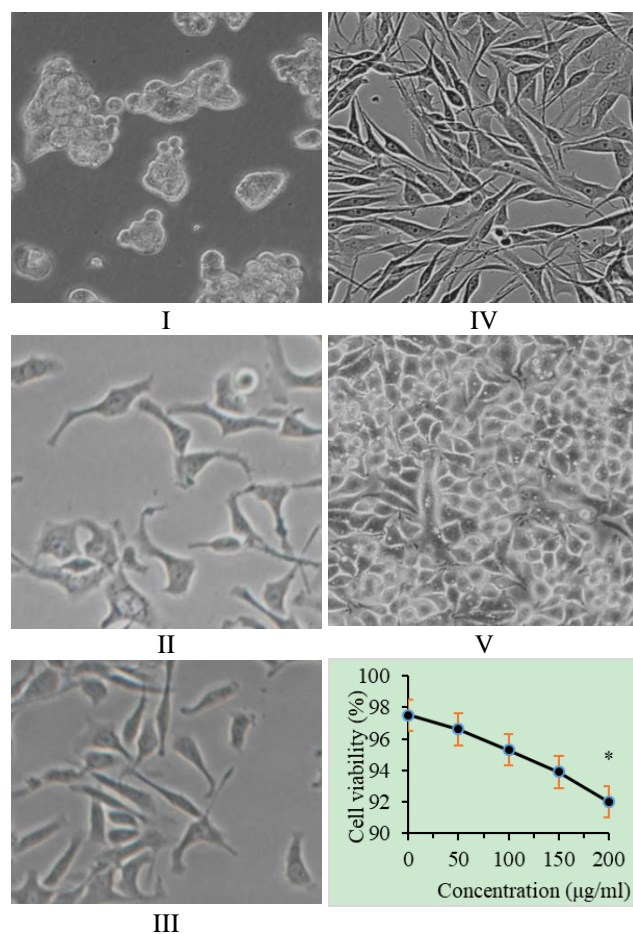


Figure 5. Influences of Yb(OH)CO₃ nanoparticles on HePG2 cell viability. (Figure I represented 0µg/mL Yb(OH)CO₃ nanoparticles, Figure II denoted 50µg/mL Yb(OH)CO₃ nanoparticles, Figure III presented 100µg/mL Yb(OH)CO₃ nanoparticles, Figure IV displayed 100µg/mL Yb(OH)CO₃ nanoparticles, and Figure V showed 200µg/mL Yb(OH)CO₃ nanoparticles. **P*<0.05 indicated that the comparison with the control group demonstrated statistical significance)

Influences of Yb(OH)CO₃ nanoparticles on mice HE staining

In the research, mice were sacrificed and their livers, lungs, and kidneys were extracted after they were raised for 1 month. HE staining was performed on the mice added with 200µg/mL Yb(OH)CO₃ nanoparticles and on the mice without being added with Yb(OH)CO₃ nanoparticles, respectively. The results of HE staining were shown in Figure 6 as follows. According to Figure 6, the tissue damage was not observed in the results of HE staining for mice tissues in two groups. Therefore, the results of HE staining indicated that the prepared Yb(OH)CO₃ nanoparticles caused no damage to mice.

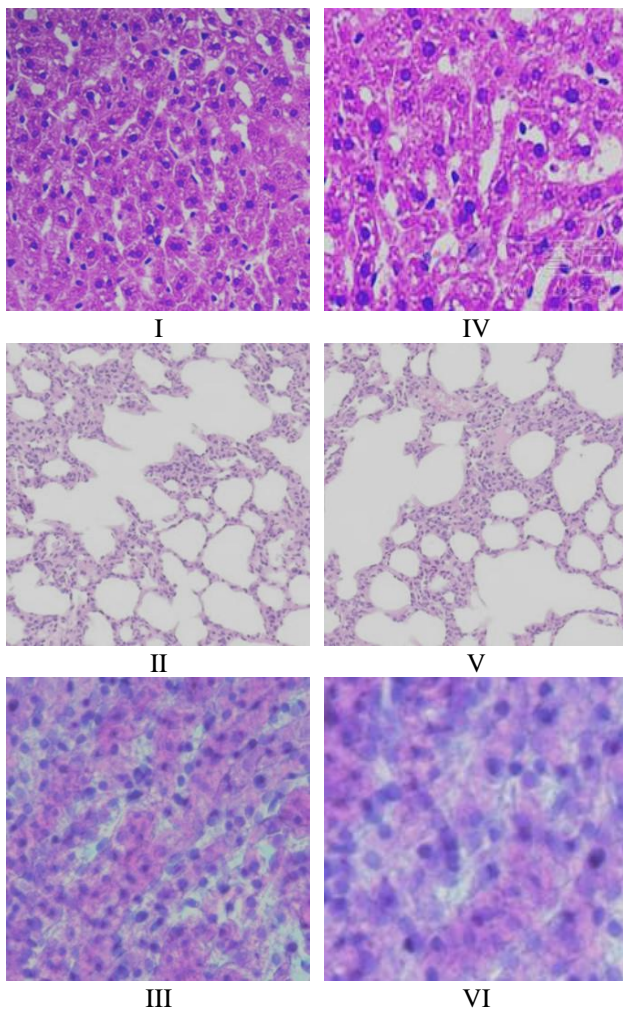


Figure 6. Results of HE staining for mice in two groups. (Figures I, II, and III represented HE staining for mice livers, lungs, and kidneys without being added with Yb(OH)CO₃ particles, respectively. Figures IV, V, and VI denoted HE staining for mice livers, lungs, and kidneys added with Yb(OH)CO₃ particles, respectively)

Results of evaluation of SVM pneumothorax prediction models

Figure 7 displayed the prediction results of LBP by SVM. According to Figure 7, the prediction accuracy of pneumothorax by SVM reached 88.7%, the sensitivity was 71.3%, and the specificity amounted to 100%. In contrast, the prediction accuracy of pneumothorax by RF was 79.8%, the sensitivity reached 74.5%, and the specificity amounted to 77.9%. The above results showed the prediction indexes of pneumothorax by SVM were significantly higher than those by the RF model, which demonstrated that the prediction performance of pneumothorax by SVM was more excellent than that by RF model. Hence, SVM could be utilized to construct a pneumothorax prediction model.

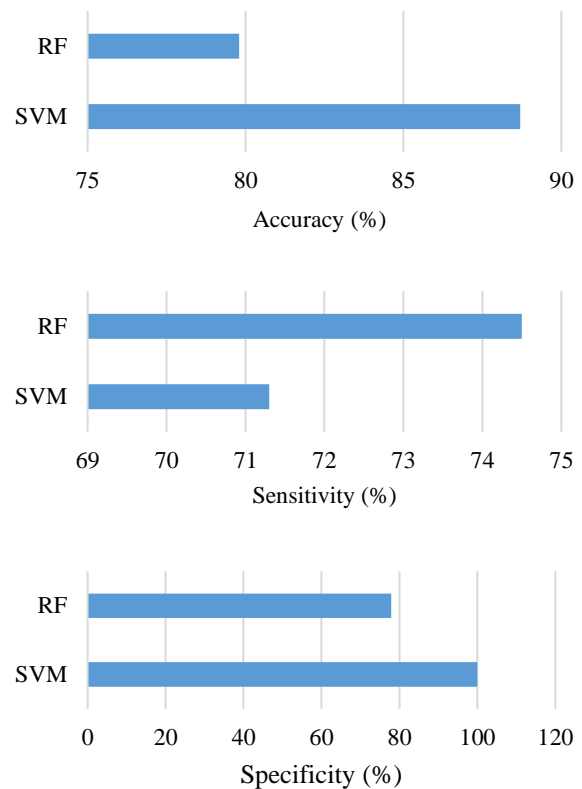


Figure 7. Prediction indexes of pneumothorax by two models.

Clinical data of all patients

A total of 40 patients receiving CT-guided PTNB were included in the research. Table 1 presented the general data on 20 patients in the control group and 20 patients in the observation group. There was no significant difference between patients in the two

groups in terms of gender, age, and body mass indexes ($P>0.05$). The above values could be utilized in subsequent comparisons. Among the included 40 patients, there were 26 males and 14 females aged between 35 and 79, and 18 out of them suffered from pneumothorax.

Table 1. General data on patients in two groups

Classification	Gender(male/female)	Age	BMI
Control group	14/6	55.4±3.7	23.4±2.9
Observation group	12/8	54.7±3.3	23.8±3.7

Evaluation indexes of CT imaging of patients in two groups

In the research, SVM was adopted to construct pneumothorax prediction models. The results of the quantitative evaluation of the CT imaging effects on patients demonstrated that the CT imaging accuracy of the observation group was 96.7%, the sensitivity reached 84.3%, and the specificity amounted to 100%. CT imaging effects on the observation group were better than those in the control group. Figure 8 displayed the evaluation indexes of CT imaging effects on patients in two groups.

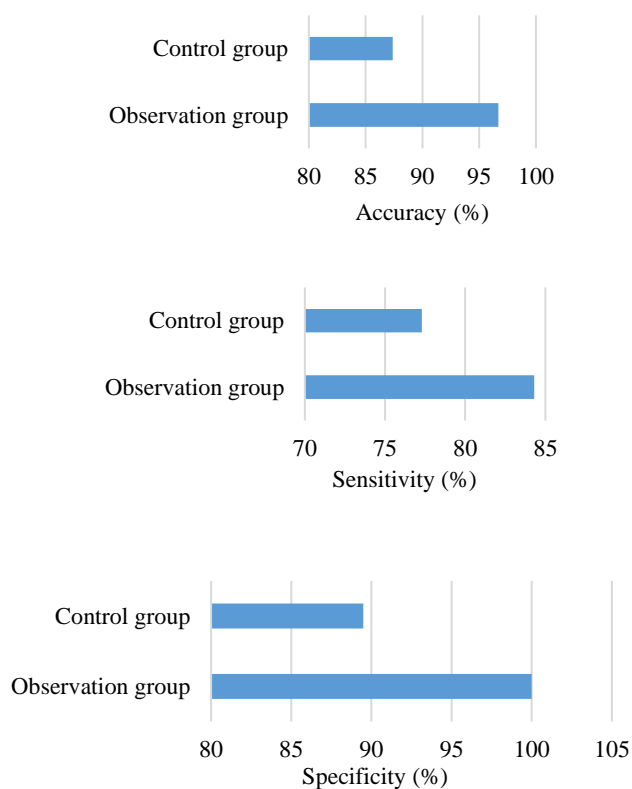


Figure 8. CT imaging evaluation indexes of patients in two groups.

Evaluations of puncture effects of different CT contrast agents on patients in two groups

Mean squared error (MSE) and MI (mutual information) were adopted to evaluate the puncture effects of contrast agents on patients in two groups, and the evaluation results of puncture effects were shown in Figure 9 below. According to Figure 9, the MSE of CT contrast agents and conventional agents of Yb(OH)CO₃ nanoparticles were 14532 and 7021, respectively, and MI was 0.1232 and 0.2354, respectively. The comparison between the two groups indicated that the differences showed statistical meaning ($P<0.05$).

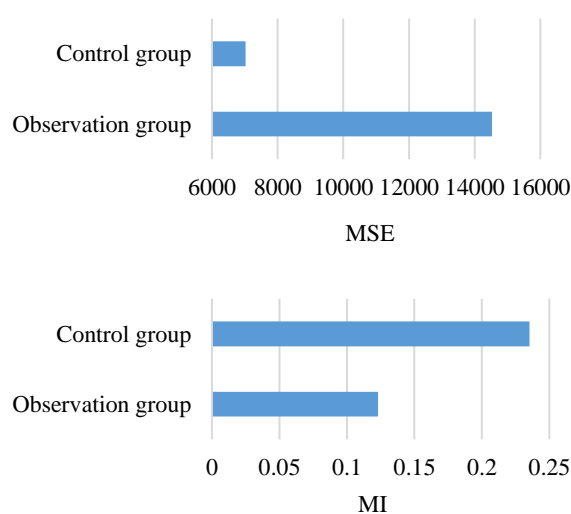


Figure 9. Evaluation indexes of puncture effects of different contrast agents on patients in two groups.

Cancer is the main disease that poses a threat to human life and health at present. World Cancer Report 2014 published latest by World Health Organization reveals that the current global incidence of cancer is constantly rising. Among all death cases, nearly 30% die from cancer. Besides, it is predicted in the report that there will be nearly 20 million new cancer patients per year in the following 20 years, and nearly 13 million death cases die from cancer every year. In China, cancer becomes the most deadly disease threatening residents. According to the statistical data released by China's Three-year Action Plan for Cancer Prevention and Treatment (2015-2017), which is published by the National Health and Family Planning Commission, the number of new cancer patients in China is about 3.1 million every year, and nearly 2 million out of them die. The current

situation of cancer prevention and treatment is very serious (17). In the detection of cancers, imaging diagnosis is adopted clinically as the result of the auxiliary diagnosis. CT scanning is one of the most widely adopted non-traumatic clinical imaging technologies because of its wide applications, relatively low price, high efficiency, and high resolution. Although the resolution of CT is far higher than that of traditional X-ray and other several imaging technologies, CT can hardly detect subtle changes in soft tissues due to the limitations of imaging principles. To enhance the contrast of soft tissues and the diagnostic accuracy of diseases, multiple CT contrast agents are developed. The CT contrast agent firstly applied clinically is small-molecule iodide. In general, materials with high density or high atomic number (Z) all can absorb X-rays, such as iodine, barium, gold, bismuth, and tantalum. All the above elements can be utilized as the contrast agents of X-ray imaging. Iodide is the earliest and the most widely used CT contrast agent in clinical practice. However, the imaging time of this contrast agent is short. In addition, the high osmotic pressure, high viscosity, and electric charge it possesses usually trigger contrast agent reactions, which jeopardize patients' lives and safety (18). As a result, its further application is restricted to a large degree due to the above shortcomings.

With the rise of nanotechnology, it is applied to CT contrast agents by researchers. Compared with traditional small-molecule contrast agents, nanoparticles can load a large number of contrast elements, nanoparticles result in long blood circulation, and low kidney clearance as well as capillary leakage. By different surface modifications, nanoparticles can also acquire the function of active targeting or treatment and multi-modal contrast. Iodine is still utilized as the contrast element in the firstly prepared nano CT contrast agent. Iodide is made into nano-emulsion or embedded into carriers to enhance blood circulation time and biocompatibility. Inorganic metallic nano contrast materials (gold, bismuth, tantalum, ytterbium, and lutetium) receive more and more attention from a wide range of researchers. Inorganic metallic nanoparticles are widely adopted in the study and application of nano CT contrast agents because of high stability, high transmittance into immune system barriers, high

density, large atomic number, and excellent biocompatibility. The element ytterbium shows a very strong imaging capacity. Freedman, et al. (2014) (19) designed, developed, and combined the binary CT imaging systems of ytterbium and barium. The composite imaging system could offer good imaging effects with CT voltage ranging between 80kVp and 140kVp, and it is adopted mainly under in vivo imaging (20). Yi, et al. (2014) (21) reported the chemical modification of polyethylene glycol to Na LuF₄: Yb/Er, which is utilized in the contrast agents of fluorescence/X-ray dual-mode imaging. The experiment proved that nanoparticles accumulated in the lung of mice at first after Na LuF₄: Yb /Er was intravenously injected into mice bodies, which caused the appearance of significantly enhanced signal shadows in the lungs firstly. After that, nanoparticles gradually gathered in livers and spleens and showed corresponding strong signal shadows. The special metabolic feature of this nano-imaging contrast agent offered a novel nano-contrast agent for CT diagnosis of lung diseases. Besides, the research was based on urea, and Yb(OH)CO₃ nanoparticles were successfully prepared by the homogeneous precipitation method, which was a classical preparation method. Based on chemical reaction and intermediate reaction products, crystalline ions were released slowly and uniformly from the solution. Furthermore, precipitates were separated uniformly. In general, there was no immediate chemical reaction between the added precipitant and the precipitated component right away. Instead, precipitant was induced to form slowly throughout the solution by external factors. Meanwhile, particle locality as well as inhomogeneity, the formation of large particle size, serious aggregation, and wide distribution of particles were avoided, all of which were caused by the uneven concentration of ions in solution in the direct precipitation method. Yb(OH)CO₃ nanoparticles prepared by the homogeneous precipitation method in the research were spherical with the average diameter being about 170nm. Besides, each Yb(OH)CO₃ nanoparticle showed a clear boundary with a smooth surface and excellent dispersibility. The above features of Yb(OH)CO₃ nanoparticles proved that Yb(OH)CO₃ nanoparticles were successfully prepared. To verify the non-toxicity of the prepared Yb(OH)CO₃ nanoparticles for cells, the in vitro and

in vivo toxicity was studied and analyzed by MTT experiment and mice experiment. The results showed that the cell viability of Yb(OH)CO₃ was still 92% 48 hours after being processed. In addition, the mice in vivo experiment confirmed that the prepared Yb(OH)CO₃ nanoparticles showed no negative influence on mice, which was similar to the published articles (22).

The complications of CT-guided percutaneous lung biopsy include pneumothorax, hemorrhage, cardiopulmonary arrest, shock, acute cardiac tamponade, mediastinal emphysema and hematoma, air embolism, and spreading of the tumor. Pneumothorax is a common complication of lung puncture biopsy, and serious pneumothorax may result in ventilation-perfusion ratio abnormality and the incidence of respiratory failure. The accurate detection of pneumothorax is the prerequisite of the quantitative assessment of pneumothorax. Because pneumothorax appears on sternums with curved outlines and smooth areas. A dark area forms at thoracic walls and ribs, and it is very easy to confuse the dark area with other tissues in the chest. The changes in the shape, size and locations of pneumothorax are significant. As a result, missed diagnosis or misdiagnosis of pneumothorax as other diseases, such as pulmonary emphysema, pulmonary bulla, and inflammatory cavity, usually occurs (23). According to the report of related articles (24), More than 70 thousand pneumothorax patients are not properly treated every year, including missed patients and those diagnosed with other diseases. In China, missed diagnosis and misdiagnosis are also common. In addition, it is also difficult to diagnose some micropneumothorax (25). Therefore, the construction of pneumothorax prediction models in advance shows excellent preventive effects on the incidence of pneumothorax. Anzidei, et al. (2015) (26) proposed the pneumothorax risk model called modulus of rupture to predict pneumothorax based on multiple risk factors. The results showed that the model could well predict the risk in the incidence of the complications of patients receiving CT-guided percutaneous lung biopsy. In the research, the SVM method was adopted to construct pneumothorax prediction models, and the results demonstrated that the prediction accuracy of pneumothorax by SVM reached 88.7%, the sensitivity was 71.3%, and the

specificity reached 100%. Besides, 40 patients with lung punctures were included in the research. The detection accuracy of CT imaging of patients in the observation group with Yb(OH)CO₃ nanoparticles reached 96.7%, the sensitivity amounted to 84.3%, and the specificity reached 100%. The above values further proved that SVM could help doctors predict the risk in the incidence of lung puncture biopsy pneumothorax automatically. To conduct the quantitative evaluation of the different imaging results of patients in two groups, two indexes including MSE and MI were adopted as the evaluation indexes. The results showed that the MSE of CT contrast agents of Yb(OH)CO₃ nanoparticles and that of conventional contrast agents were 14532 and 7021, respectively. Besides, MI of the above two contrast agents were 0.1232 and 0.2354, respectively. The comparison between the two groups revealed that the differences showed significant meaning ($P < 0.05$).

Conclusions

Yb(OH)CO₃ nanoparticles adopted in CT imaging were successfully prepared based on urea in the research. The prepared Yb(OH)CO₃ nanoparticles showed excellent histocompatibility and low toxicity. In addition, CT imaging of Yb(OH)CO₃ nanoparticles demonstrated high accuracy in lung puncture biopsy pneumothorax prediction models. However, there were still some disadvantages. For example, whether the prepared Yb(OH)CO₃ nanoparticles would be toxic to the human body if the retention time of Yb(OH)CO₃ in vivo was long. In future research, a more detailed study on this issue would be carried out. To conclude, the research provided the reference basis for the adoption of Yb(OH)CO₃ nanoparticles as the new CT contrast agents.

Acknowledgments

Not applicable.

Interest conflict

The authors declare that they have no conflict of interest.

References

1. Jemal A, Bray F, Center MM, et al. Global cancer statistics. *CA Cancer J Clin.* 2011 Mar-Apr;61(2):69-90. doi: 10.3322/caac.20107. Epub 2011 Feb 4. Erratum in: *CA Cancer J Clin.* 2011 Mar-

- Apr;61(2):134. PMID: 21296855.
2. Jemal A, Siegel R, Ward E, et al. Cancer statistics, 2009. *CA Cancer J Clin.* 2009 Jul-Aug;59(4):225-49. doi: 10.3322/caac.20006. Epub 2009 May 27. PMID: 19474385.
 3. Jemal A, Siegel R, Ward E, et al. Cancer statistics, 2008. *CA Cancer J Clin.* 2008 Mar-Apr;58(2):71-96. doi: 10.3322/CA.2007.0010. Epub 2008 Feb 20. PMID: 18287387.
 4. Allemani C, Weir HK, Carreira H, et al. Global surveillance of cancer survival 1995-2009: analysis of individual data for 25,676,887 patients from 279 population-based registries in 67 countries (CONCORD-2). *Lancet.* 2015 Mar 14;385(9972):977-1010. doi: 10.1016/S0140-6736(14)62038-9. Epub 2014 Nov 26. Erratum in: *Lancet.* 2015 Mar 14;385(9972):946. PMID: 25467588; PMCID: PMC4588097.
 5. Torre LA, Bray F, Siegel RL, et al. Global cancer statistics, 2012. *CA Cancer J Clin.* 2015 Mar;65(2):87-108. doi: 10.3322/caac.21262. Epub 2015 Feb 4. PMID: 25651787.
 6. Bray F, Ferlay J, Soerjomataram I, et al. Global cancer statistics 2018: GLOBOCAN estimates of incidence and mortality worldwide for 36 cancers in 185 countries. *CA Cancer J Clin.* 2018 Nov;68(6):394-424. doi: 10.3322/caac.21492. Epub 2018 Sep 12. Erratum in: *CA Cancer J Clin.* 2020 Jul;70(4):313. PMID: 30207593.
 7. Feng RM, Zong YN, Cao SM, et al. Current cancer situation in China: good or bad news from the 2018 Global Cancer Statistics? *Cancer Commun (Lond).* 2019 Apr 29;39(1):22. doi: 10.1186/s40880-019-0368-6. PMID: 31030667; PMCID: PMC6487510.
 8. Pastorino U. Early detection of lung cancer. *Respiration*, 2006;73(1):5-13.
 9. National Lung Screening Trial Research Team, Aberle DR, Adams AM, et al. Reduced lung-cancer mortality with low-dose computed tomographic screening. *N Engl J Med.* 2011 Aug 4;365(5):395-409. doi: 10.1056/NEJMoa1102873. Epub 2011 Jun 29. PMID: 21714641; PMCID: PMC4356534.
 10. Tsukada H, Satou T, Iwashima A, et al. Diagnostic accuracy of CT-guided automated needle biopsy of lung nodules. *AJR Am J Roentgenol.* 2000 Jul;175(1):239-43. doi: 10.2214/ajr.175.1.1750239. PMID: 10882279.
 11. Nasrollahzadeh M. Advances in Magnetic Nanoparticles-Supported Palladium Complexes for Coupling Reactions. *Molecules.* 2018 Oct 4;23(10):2532. doi: 10.3390/molecules23102532. PMID: 30287773; PMCID: PMC6222409.
 12. Barick KC, Singh S, Bahadur D, et al. Carboxyl decorated Fe₃O₄ nanoparticles for MRI diagnosis and localized hyperthermia. *J Colloid Interface Sci.* 2014 Mar 15;418:120-5. doi: 10.1016/j.jcis.2013.11.076. Epub 2013 Dec 5. PMID: 24461826.
 13. Au JT, Craig G, Longo V, et al. Gold nanoparticles provide bright long-lasting vascular contrast for CT imaging. *AJR Am J Roentgenol.* 2013 Jun;200(6):1347-51. doi: 10.2214/AJR.12.8933. PMID: 23701074.
 14. Ferrari M. Nanotechnology: opportunities and challenges. *Nat Rev Cancer*, 2005,(5),161-171.
 15. Lusic H, Grinstaff MW. X-ray-computed tomography contrast agents. *Chem Rev.* 2013 Mar 13;113(3):1641-66. doi: 10.1021/cr200358s. Epub 2012 Dec 5. PMID: 23210836; PMCID: PMC3878741.
 16. Rabin O, Manuel Perez J, Grimm J, et al. An X-ray computed tomography imaging agent based on long-circulating bismuth sulphide nanoparticles. *Nat Mater.* 2006 Feb;5(2):118-22. doi: 10.1038/nmat1571. Epub 2006 Jan 29. PMID: 16444262.
 17. Ding J, Chen L, Xiao C, et al. Noncovalent interaction-assisted polymeric micelles for controlled drug delivery. *Chem Commun (Camb).* 2014 Oct 7;50(77):11274-90. doi: 10.1039/c4cc03153a. PMID: 25005913.
 18. Singh J, Daftary A. Iodinated contrast media and their adverse reactions. *J Nucl Med Technol.* 2008 Jun;36(2):69-74; quiz 76-7. doi: 10.2967/jnmt.107.047621. Epub 2008 May 15. PMID: 18483141.
 19. Freedman JD, Lusic H, Snyder BD, et al. Tantalum oxide nanoparticles for the imaging of articular cartilage using X-ray computed tomography: visualization of ex vivo/in vivo murine tibia and ex vivo human index finger cartilage. *Angew Chem Int Ed Engl.* 2014 Aug 4;53(32):8406-10. doi: 10.1002/anie.201404519. Epub 2014 Jun 30. PMID: 24981730; PMCID: PMC4303344.
 20. Liu Y, Ai K, Liu J, et al. A high-performance ytterbium-based nanoparticulate contrast agent for in vivo X-ray computed tomography imaging. *Angew Chem Int Ed Engl.* 2012 Feb 6;51(6):1437-42. doi: 10.1002/anie.201106686. Epub 2011 Dec 30. PMID: 22223303.
 21. Yi Z, Lu W, Xu Y, et al. PEGylated NaLuF₄: Yb/Er upconversion nanophosphors for in vivo synergistic fluorescence/X-ray bioimaging and long-lasting, real-time tracking. *Biomaterials.* 2014 Dec;35(36):9689-97. doi: 10.1016/j.biomaterials.2014.08.021. Epub 2014 Aug 29. PMID: 25176069.
 22. Xu Z, Ma P, Li C, et al. Monodisperse core-shell structured up-conversion Yb(OH)CO₃@YbPO₄:Er³⁺ hollow spheres as drug carriers. *Biomaterials.* 2011 Jun;32(17):4161-73. doi: 10.1016/j.biomaterials.2011.02.026. Epub 2011 Mar 23. PMID: 21435712.
 23. O'Connor AR, Morgan WE. Radiological review of pneumothorax. *BMJ.* 2005 Jun 25;330(7506):1493-7. doi: 10.1136/bmj.330.7506.1493. PMID: 15976424; PMCID: PMC558461.
 24. Swierzy M, Helmig M, Ismail M, et al. Pneumothorax [Pneumothorax]. *Zentralbl Chir.* 2014 Sep;139 Suppl 1:S69-86; quiz S87. German. doi: 10.1055/s-0034-1383029. Epub 2014 Sep 29. PMID: 25264729.
 25. Imran JB, Eastman AL. Pneumothorax. *JAMA.* 2017 Sep 12;318(10):974. doi: 10.1001/jama.2017.10476. PMID: 28898380.

26. Anzidei M, Sacconi B, Fraioli F, et al. Development of a prediction model and risk score for procedure-related complications in patients undergoing percutaneous computed tomography-guided lung biopsy. *Eur J Cardiothorac Surg.* 2015 Jul;48(1):e1-6. doi: 10.1093/ejcts/ezv172. Epub 2015 May 16. PMID: 25983080.